

ANALYSIS OF MINERAL-RICH SUSPENDED MATTER IN GLACIAL LAKES USING SIMULATIONS AND SATELLITE DATA

Eder, E. ⁽¹⁾, Dörnhöfer, K. ⁽²⁾, Gege, P. ⁽³⁾, Schenk, K. ⁽⁴⁾, Klinger, Ph. ⁽⁴⁾, Wenzel, J. ⁽⁴⁾, Oppelt, N. ⁽²⁾, Gruber, N. ⁽¹⁾

⁽¹⁾ETH Zürich, Institute of Biogeochemistry and Pollutant Dynamics, Universitätstrasse 16, 8092 Zürich (Switzerland)
Email: elisabeth.eder@usys.ethz.ch, nicolas.gruber@env.ethz.ch

⁽²⁾Kiel University, Department of Geography, Ludewig-Meyn-Str.14, 24098 Kiel (Germany)
Email: doernhoefer@geographie.uni-kiel.de, oppelt@geographie.uni-kiel.de

⁽³⁾Deutsches Zentrum für Luft- und Raumfahrt (DLR), Münchener Straße 20, 82234 Weßling (Germany)
Email: peter.gege@dlr.de

⁽⁴⁾EOMAP, Schlosshof 4a, 82229 Seefeld (Germany)
Email: schenk@eomap.de, klinger@eomap.de, wenzel@eomap.de

ABSTRACT

The contribution of *mineral-rich suspended matter* (MSM) to the optics of water bodies is still less treated by bio-optical modeling than that of other water constituents. However, with the increasing number of remote sensing studies on inland waters, optical properties of terrestrial particles gain importance for accurately estimating particle concentrations. We compared two current simulation tools, *Hydrolight* and *WASI*, for high MSM concentrations within the realistic context of catchments with glacial erosion. The study area is an extreme form of suspended sediment-dominated *Case2* water. We simulated $R_{rs}(0-)$ spectra with MSM concentrations varying from 5 to 200 g m⁻³. In a second step, *WASI-2D* was applied to invert *Landsat8*. In-situ measured concentrations and reflectance spectra served to assess model performance. Thus, we tested the suitability of the analytical model *WASI* for high MSM concentrations and point out necessities for future adaptations to (extremely) turbid environments.

1. INTRODUCTION

Mineral-rich suspended matter (MSM) is a main optical component of many inland waters, especially those characterized by high terrestrial influence. High MSM concentrations in areas of river intrusion, land erosion and bottom resuspension cause reflectance values to shoot up, impairing the water's light regime with possible ecological consequences. During field studies in lakes located in catchments dominated by glacial erosion in the Swiss Alps, we encountered MSM concentrations at the surface water layer of up to ~200 g m⁻³. We found low absorptive, highly scattering *glacial flour* that caused high reflectance values throughout the visible and near infrared domain [1].

In front of the challenging optical properties of this type of water, we tested two software tools that are commonly used in the scientific community of aquatic remote sensing: *Hydrolight* (Sequoia Scientific, Inc.), in the following abbreviated as HE, and *WASI* (Water Colour Simulator) by Gege [2]. HE is a commercial tool which numerically solves the equation of radiative transfer in natural waters, as described in [3], to generate reflectance spectra (*forward simulation*). It requires information on the absorption properties and the angular distribution of scattering properties of the water constituents.

WASI is a free-of-charge tool (download at <http://www.ioccg.org/data/software.html>) that solves an analytical model which refers to the model developed by [4, 5]. The objective of Albert's work was to find a set of analytical equations to generate spectra of natural water bodies that are similar to the elaborate, numeric HE simulations, i.e. the analytical equations are approximations of the radiative transfer equations [5]. The basic equation used for subsurface radiance reflectance, is [Eq.(1)]:

$$Rrs(0-) = f_{rs} \frac{b_b}{a + b_b} \quad (1)$$

with a [m⁻¹] being the sum of absorption coefficients, and, respectively, b_b [m⁻¹] being the sum of backscattering coefficients of all water compounds. f_{rs} was parametrized by a polynomial function using the coefficients reported in [4].

The analytical functions were empirically parametrized by analysis of a set of HE simulated spectra (400 to 750 nm) of water bodies with varying concentrations of water constituents. The optical properties of the water constituents referred to measurements at *Lake Constance*, Germany, an oligo- to mesotrophic pre-

Alpine inland water. The range of suspended particle concentrations considered in the reference spectra is covered up to 50 g m^{-3} , but the number of cases with $< 10 \text{ g m}^{-3}$ is disproportionately high [4]. The analytical model requires only the absorption and backscattering properties of the water compounds.

Besides the model by [4, 5], WASI provides further model options (see WASI4 manual), which, however, had not been tested in the present work. The software tool allows both forward simulations and inversion of spectra, even of two-dimensional data (WASI-2D).

In the following, we test the suitability of Albert's model as implemented in WASI for high concentrations of MSM within the referenced range up to 50 g m^{-3} , and beyond that up to 200 g m^{-3} . The theoretical study is supplemented by the practical application of WASI-2D for constituent retrieval based on satellite data. For this, we first use HE forward simulations to inversely retrieve *inherent optical properties* (IOPs) [6] from *Landsat8* data. In the second step, a *Landsat8* scene is inverted in WASI-2D based on the optimized parameters in terms of MSM and *colored dissolved organic matter* (CDOM, or *gelbstoff*). Results of the models are compared with in-situ data.

2. STUDY SITE

Fig.1 shows the study area *Räterichsbodensee*, which is one of the major pumped-storage (PS) operated reservoirs located in the *Grimsel Massif*, central Switzerland, located on $\sim 1790 \text{ m asl}$. Due to PS the water level alternates drastically with high values ($\sim 70 \text{ m}$) in autumn and low values ($\sim 7 \text{ m}$) in early spring. The upper located glacier-fed reservoirs (*Oberaarsee*, *Grimselsee*) discharge their particle-rich water into *Räterichsbodensee* which would otherwise be fed only by snow melt and rain. The surface discharge causes a milky-greenish appearance of the surface water. Owing to glacier melt, heavy precipitations in summer and the anthropogenic influence MSM concentrations vary seasonally with, in tendency, increasing concentrations by the end of season. In spite of the strong light attenuation primary production had been detected to grow in early autumn [1].

3. METHODS

3.1 Theoretical comparison HE vs. WASI

Spectra were generated with both models for waters containing MSM concentrations from 5 to 200 g m^{-3} using absorption and backscattering properties found typical for *Grimsel glacial flour* [1] (but could have been performed also with *any* other a_p^* and b_{bp}^* values). All other water compounds (phytoplankton, CDOM) were set to zero. No inelastic light sources were allowed. The bottom condition was set to infinitely

deep. Absorption and scattering properties of pure fresh water were taken from the HE default data file. All atmospheric conditions were kept equal (sun zenith 30° , wind speed 0 m s^{-1}).

To perform simulations in WASI in a way compatible with the HE simulations, we set the concentration of phytoplankton, [C_0], equal to the concentration of particles Type I, [C_X] (for nomenclature see WASI4 manual). This setting allows reading absorption and backscattering properties of suspended particles from file.

3.2 In-situ and satellite data

The reservoir *Räterichsbodensee* was studied by an in-situ campaign on 2014, July 3rd. At 11 sites along the length axis of the reservoir (Fig.1) surface water was sampled and analyzed in terms of MSM by gravimetric estimation using GF/F filters (Whatmann). Sampling was accompanied by measurements of radiance reflectance just above water, $R_{rs}(0+)=Lu(0+)/Ed(0+)$ [sr^{-1}], from a self-constructed catamaran. Spectra were corrected for sun glint applying the correction scheme by Ruddick et al. [7, 8], and subsequently converted to $R_{rs}(0-)$ using the algorithm by Lee et al. [9]. Two hours before sampling, *Landsat8* acquired a scene. The *Landsat8* data were atmospherically corrected using the MIP algorithm by Heege et al. [10] delivering radiance reflectance just beneath surface, $R_{rs}(0-)=Lu(0-)/Ed(0-)$ [sr^{-1}]. Only 7 of the 11 measured sites could be captured by satellite while the others (sites 1, 9, 10, 11, Fig.1) were located too close to the shore.

3.3 Inverse retrieval of IOPs using Hydrolight

Since no IOPs had been collected for this campaign, experimental results from previous campaigns were used and supplemented by parameters retrieved *inversely by look-up table* [11]. We used measurements of the mass-specific particulate backscattering coefficient, b_{bp}^* [$\text{m}^2 \text{ g}^{-1}$] collected in previous studies [1]. Absorption by CDOM, a_g [m^{-1}], and mass-specific particulate absorption, a_p^* [$\text{m}^2 \text{ g}^{-1}$] were retrieved by spectrum matching of simulated spectra with the median of the $R_{rs}(0-)$ spectra by *Landsat8*. Since the spectra along the reservoir showed almost no variation (see RESULTS below) the median had been chosen to be appropriate for spectrum matching. The concentration of phytoplankton was set to zero. Simulations were performed with HE Version 5.0. Simulated spectra were resampled to the FWHM of the first five *Landsat8* bands prior to spectrum matching. Despite high similarity in the measured reflectance spectra, the estimated MSM values spanned a range of 17 g m^{-3} (see RESULTS below). Thus, we also included the MSM value into the optimization varying its value within the measured range.

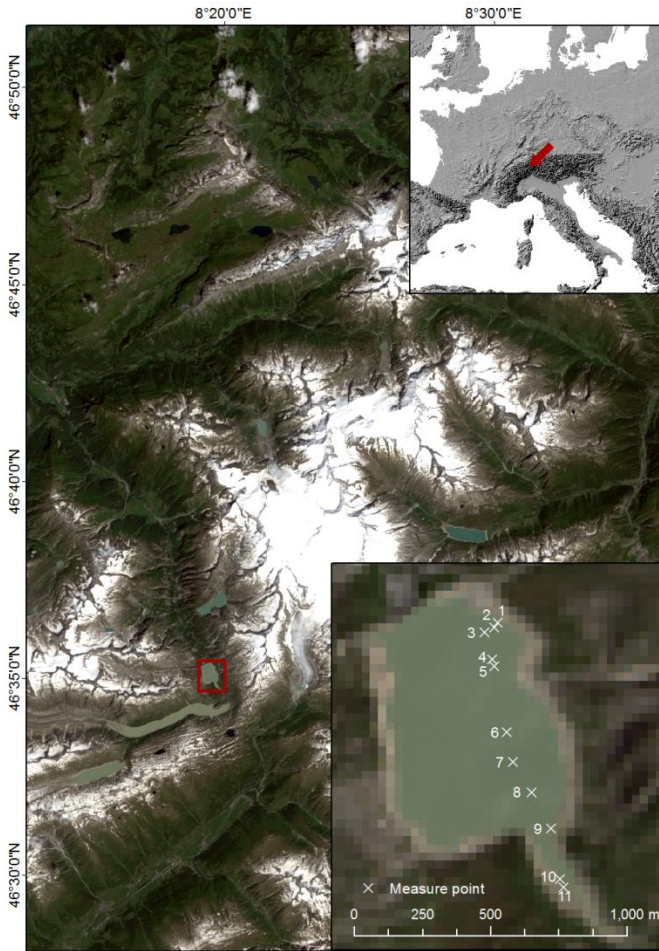


Figure 1. Study area Räterichsbodensee. Background: Landsat 8 true-colour composite, acquisition date: July 3rd 2014 (Source: USGS 2014: Landsat 8 dataset. <http://earthexplorer.usgs.gov/>; EEA 2010: Elevation Map Europe. European Environment Agency)

3.4 Inversion of Landsat8 scene in WASI-2D

The Landsat8 scene was inverted by WASI-2D to retrieve MSM concentrations. For this, WASI-2D tries to model the $R_{rs}(0-)$ spectrum of each pixel included in the Landsat8 scene as close as possible. All spectral input is comprised in the bands 1 (440 nm), 2 (480 nm), 3 (560 nm), 4 (655 nm) and 5 (865 nm). Specific absorption and backscattering properties were parameterized according to the results of the HE optimization (see section 3.3). Inversion was performed based on the models of R_{rs} and f_{rs} specified in Eq. (1). During inversion, WASI-2D varies variable parameters within a pre-defined range until modelled and satellite-measured spectra achieve best correspondence. Besides MSM also a_g was included as a variable parameter in the WASI inversion to increase the degree of freedom. To implement the absorption and backscattering properties of suspended glacial flour we used the model configuration as described above (section 3.1).

4. RESULTS AND DISCUSSION

4.1 Theoretical comparison HE vs. WASI

The $R_{rs}(0-)$ spectra (Fig.2a), simulated with WASI within the reference MSM range $< 50 \text{ g m}^{-3}$, showed higher values compared to HE simulations. The relative error (Fig.2b) increased with increasing water clarity within the referenced wavelength range 400 to 750 nm but increased above $> 750 \text{ nm}$ with increasing turbidity. For $\text{MSM} > 50 \text{ g m}^{-3}$ (Fig.3a) the situation was different. The relative error (Fig.3b) was decreasing with increasing MSM concentration. Differences mainly occurred in the near-infrared. WASI and, respectively, HE spectra for different MSM concentrations are congruent up to $\sim 500 \text{ nm}$ since the theoretical scenarios miss other absorbing components (phytoplankton, CDOM) that are typically found in natural waters to some degree.

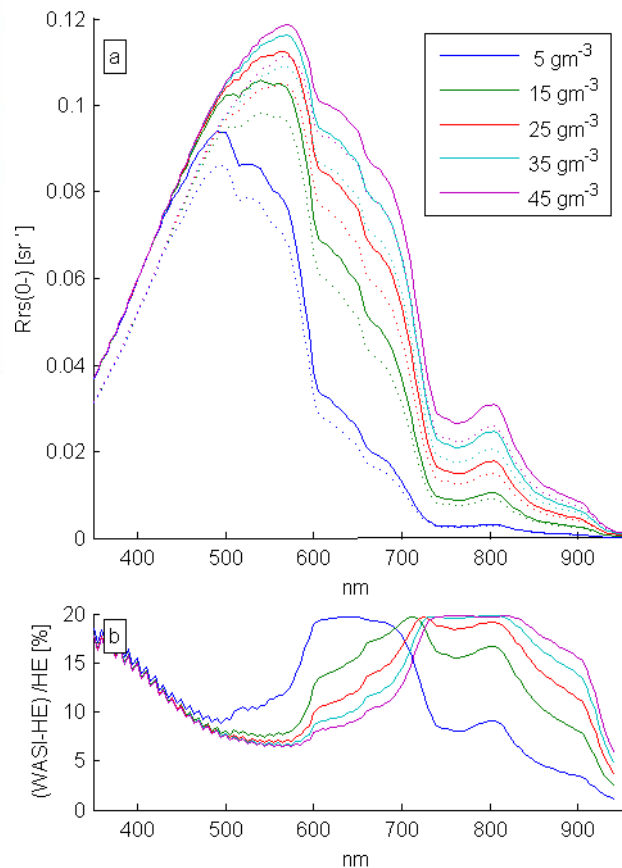


Figure 2. a: Comparison of forward simulated $R_{rs}(0-)$ spectra with WASI (solid line) and HE (dashed line) for $\text{MSM} < 50 \text{ g m}^{-3}$. b: Relative error of WASI compared to HE spectra

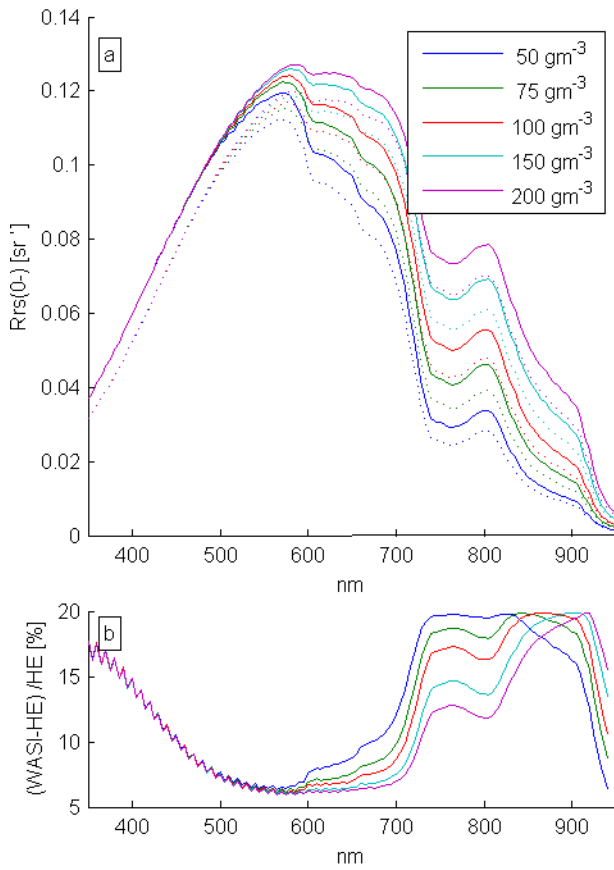


Figure 3. a: Comparison of forward simulated $R_{rs}(0-)$ spectra with WASI (solid line) and HE (dashed line) for $>50 \text{ g m}^{-3}$. b: Relative error of WASI compared to HE spectra

4.2 Measurements (MSM, reflectance)

In-situ measured spectra agreed well with atmospherically corrected *Landsat8* spectra (Fig.4). Satellite-derived $R_{rs}(0-)$ were within or close to the 25% and 75% percentiles on in-situ spectra. Both in-situ and satellite spectra of the 11 and, respectively, 7 sites showed almost no variation indicating that the reservoir along the measurement sites must have been already relatively homogenized at the time of measurement. The measured MSM concentrations at the 11 sites varied between 35 to 52 g m^{-3} . The highest value was measured at site 11, the inflow from the upper reservoirs. But besides that no clear distribution along a spatial gradient could be identified. The result points out the difficulty to detect comparably small differences of MSM concentrations if the reflectance in the short and visible wavelengths is already very high. At high MSM concentrations and especially on small and patchy waters analyses of water samples can only be an indicator for the expected order of magnitude.

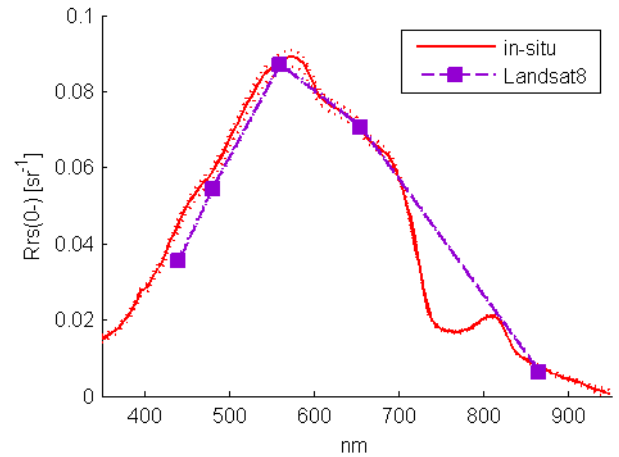


Figure 4. R_{rs} spectra: median \pm 25% and 75% percentiles of in-situ (11 sites) and *Landsat8* (7 sites)

4.3 Inverse retrieval of IOPs using Hydrolight

The HE runs supported the previously measured $b_{bp}^*(550)$ of $0.0203 \text{ m}^2 \text{ g}^{-1}$ [1] to be correct. From matching with 10.080 simulated spectra (Fig.5) we further retrieved the following IOPs: $a_p^*(440)$ being $0.048 \text{ m}^2 \text{ g}^{-1}$ with the slope being 0.015 nm^{-1} , and $a_g(440)$ being 0.5 m^{-1} with the slope being 0.013 nm^{-1} . The best fit was reached with spectra having a MSM of 35 g m^{-3} , which is at the lower end of the range of in-situ measured MSM concentrations.

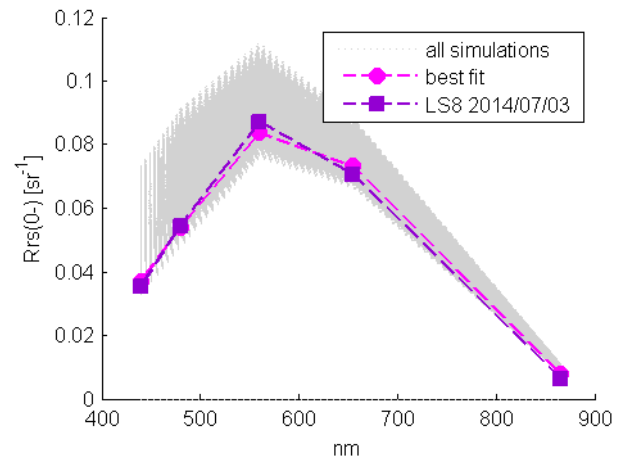


Figure 5. Spectrum matching of simulated $R_{rs}(0-)$ spectra (HE) with the median *Landsat8* spectrum

4.4 Inversion of *Landsat8* scene in WASI-2D

Fig.6 illustrates results of the WASI inversion based on *Landsat8*. The inverted MSM concentration spanned a range from 23 to 31 g m^{-3} . The inverted $a_g(440)$ ranged between 0.36 and 0.94 m^{-1} . The low MSM values and, respectively, high a_g values along the shoreline may be due to mixed pixels close to the land-water border. These pixels also showed high residuals

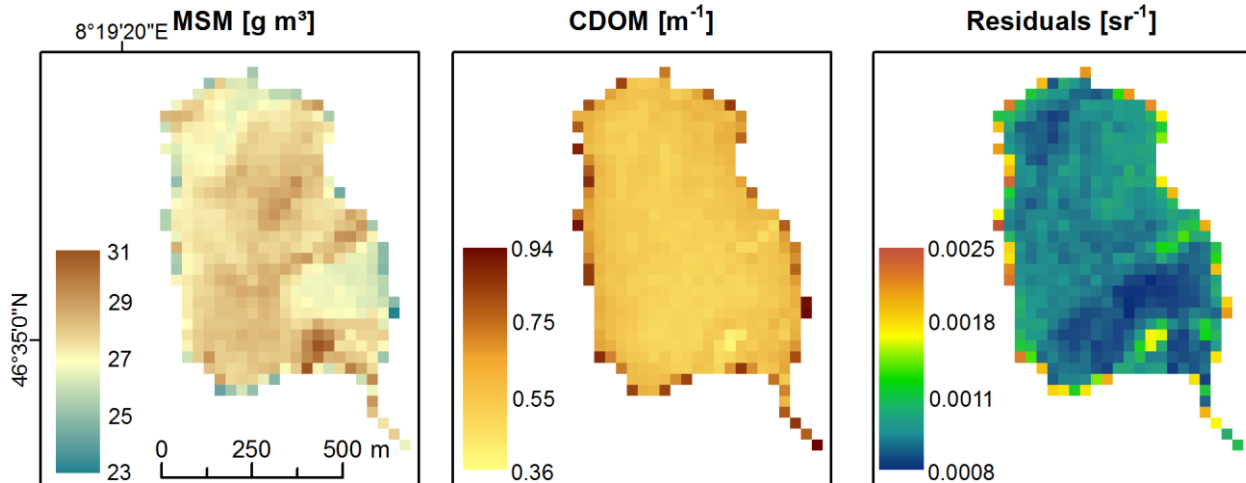


Figure 6. (left) spatial distribution of MSM and (middle) CDOM resulting from inversion of the Landsat8 imagery using WASI. (right) residual [sr^{-1}] between WASI-simulated and measured spectrum

between measured *Landsat8* and inversely modelled spectra. The retrieved concentrations ranged between ~ 25 and 31 g m^{-3} MSM, and, respectively, 0.36 to $\sim 0.75 \text{ m}^{-1} a_g(440)$. The absolute residuals between the satellite spectra and the inverted spectra were less than 0.0018 sr^{-1} (excluding the border pixels). The average (std. dev.) retrieved MSM at the seven satellite detected sites was $28 (0.70) \text{ g m}^{-3}$. Thus, the model inversion error accounts for 20% of the value supported by HE simulations (35 g m^{-3}).

A model inversion error of 10% had been reported for WASI [5] for suspended particle concentrations $< 10 \text{ g m}^{-3}$. In general, the particle concentration is underestimated by the model due to model approximations.

5. CONCLUSION

Application of the analytical model by [4, 5] as implemented in WASI to waters highly affected by terrestrial particles is possible. Forward simulations with WASI overestimated $R_{rs}(0^-)$ reflectance (400 – 750 nm) relative to numeric HE simulations. Overestimations increased with increasing water clarity within the referenced particle concentrations $< 50 \text{ g m}^{-3}$ but decreased for $> 50 \text{ g m}^{-3}$. Application of WASI-2D on a *Landsat8* scene yielded 20% lower MSM values than inverse retrieval using HE simulations supported. Still, the WASI inversion result can be accepted considering that the original model by [4, 5] was not intended to be applied to this kind of water. First, the model actually allows non-algal particles to only scatter light. The model version implemented in WASI further introduced another kind of non-algal particles, detritus [C_D], to absorb light but not to scatter light. The only way to make WASI simulations and inversions work the

way HE does is to set MSM equal to the concentration of phytoplankton, [C_0], whose absorption and backscattering properties then are read from file. However, the presented setting is no longer possible if besides absorbing and scattering particles also absorbing and scattering phytoplankton, e.g. diatoms, affect the optics of the water. Second, the analytical model was originally set up for water types with particle concentrations mainly $< 10 \text{ g m}^{-3}$ and stronger influenced by phytoplankton and CDOM. Adaptation of WASI to (extremely) turbid environments like the glacier-fed type of water we presented here requires a specific parameterization of the implemented analytical functions that considers the optical properties of terrestrial particles.

6. REFERENCES

1. Eder, E., *Estimation of total suspended matter in glacial-flour rich (sub-)Alpine reservoirs by hyperspectral data: characterization of optical properties of water constituents and water bodies by lab measurements, in-situ measurements, radiative transfer modeling and remotely sensed data*. Ph.D. Dissertation, Swiss Federal Institute of Technology in Zurich (ETHZ), Switzerland. (in progress). 2016.
2. Gege, P., *WASI-2D: A software tool for regionally optimized analysis of imaging spectrometer data from deep and shallow waters*. Computers & Geosciences, 2014. **62**: p. 208-215.
3. Mobley, C.D., *Light and Water: Radiative Transfer in Natural Waters*. 1994, San Diego, CA Academic Press. 592.
4. Albert, A. and C. Mobley, *An analytical model*

for subsurface irradiance and remote sensing reflectance in deep and shallow case-2 waters. Optics Express, 2003. **11**(22): p. 2873-2890.

5. Albert, A., *Inversion technique for optical remote sensing in shallow water.* Ph.D. Dissertation, Universität Hamburg, Germany, 188pp. 2004.
6. Preisendorfer, R.W., *Application of radiative transfer theory to light measurements in the sea.* IUGG Monographs, 1961. **10**: p. 11-30.
7. Ruddick, K., V. De Cauwer, and B. Van Mol, *Use of the near infrared similarity reflectance spectrum for the quality control of remote sensing data.* Proceedings of the SPIE - The International Society for Optical Engineering, 2005. **5885**(1): p. 588501-1-12.
8. Ruddick, K.G., et al., *Seaborne measurements of near infrared water-leaving reflectance: The similarity spectrum for turbid waters.* Limnology and Oceanography, 2006. **51**(2): p. 1167-1179.
9. Lee, Z., K.L. Carder, and R.A. Arnone, *Deriving inherent optical properties from water color: a multiband quasi-analytical algorithm for optically deep waters.* Applied Optics, 2002. **41**(27): p. 5755-5772.
10. Heege, T., et al., *Operational multi-sensor monitoring of turbidity for the entire Mekong Delta.* International Journal of Remote Sensing, 2014. **35**(8): p. 2910-2926.
11. Mobley, C.D., et al., *Interpretation of hyperspectral remote-sensing imagery by spectrum matching and look-up tables.* Applied Optics, 2005. **44**(17): p. 3576-3592.